

Flutter Prediction of a Laminar Airfoil Using a Doublet Lattice Method Corrected by Experimental Data

Anne Hebler and Reik Thormann

Abstract In this paper a stability analysis of a laminar airfoil is presented and compared to turbulent flow conditions. The flutter system with the two degrees-of-freedom heave and pitch is introduced. The aerodynamic derivatives due to a pitch motion are identified experimentally and two Doublet Lattice correction methods are used to determine the aerodynamic derivatives due to a heave motion. The correction is applied to the local pressure distributions and includes nonlinearities due to transonic flow as well as transitional effects. The resulting aerodynamic derivatives reflect the differences between laminar and turbulent flow as measured in the experiment. An influence of the mean angle-of-attack on the stability boundary is shown for free transition. A comparison of the flutter boundaries for free and fixed transition exhibits a lower transonic dip for free transition. One-degree-of-freedom flutter is found only for free transition.

1 Introduction

Energy-efficiency and environmental friendliness are important design criteria in the development of modern transport aircraft. Laminar airfoils and hybrid laminar flow control technologies have become a matter of interest, because considerable drag reductions are estimated due to laminar flow on the wing. However the influence on the aeroelastic behavior, especially on the flutter stability, is still an open point of research. Flow characteristics change significantly in comparison to modern supercritical airfoils. Therefore an investigation into the flutter behavior of a laminar airfoil in the transonic flow regime is necessary.

A. Hebler (✉) · R. Thormann
DLR, Institute of Aeroelasticity, Göttingen, Germany
e-mail: anne.hebler@dlr.de

R. Thormann
e-mail: reik.thormann@dlr.de

In a previous wind tunnel experiment, forced pitch oscillations of a CAST 10-2 airfoil model were investigated under flow with free transition and fully turbulent flow. The investigation of subsonic and moderate transonic test cases, with the main focus on the boundary layer transition process, revealed that the transition region can cover about 40% of the chord length [8]. Also it is influenced by the presence of a compression shock [8]. Nonlinearities in the steady-state behavior of the aerodynamic forces for flow with free transition were observed for the transonic flow regime [7]. Additionally, significant differences in the motion-induced unsteady airloads between flow with free transition and fully turbulent flow have been found.

The flutter problem of a laminar airfoil has been addressed with the help of computational fluid dynamics (CFD). In [10] TAU-computations, using the e^N -method for transition prediction, were performed and the flutter boundary was determined with the k-method. For laminar flow the transonic dip is deeper and is shifted to lower Mach-numbers compared to fully turbulent flow. Similar results were reported in [6], using the $\gamma - Re_\theta$ transition model, which accounts for an intermittency region.

Although these investigations provide references on the global effects of flow with free transition on the stability boundary, the aim of the present paper is to provide an additional method, which is fast but still accounts for flow nonlinearities. The flutter stability is analyzed using the results of the forced-motion experiment as the basis. Forced heave oscillations have not been measured due to technical limitations. Thus, the aerodynamic derivatives of the heave motion have to be obtained numerically. This is carried out using the Doublet Lattice Method (DLM), a panel method solving the linear unsteady aerodynamic theory in the frequency domain [1].

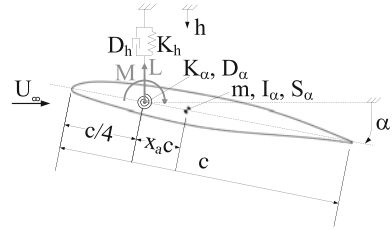
In preparation of a follow-up flutter experiment, this time with heave and pitch degree-of-freedom (DoF) allowed to respond freely, a flutter stability analysis is carried out for flow with free transition and for fully turbulent flow. On the one hand this stability analysis serves as a basis for the selection of the optimal measurement points and on the other hand it reduces the risk of damage during the experiment.

2 Approach

2.1 Flutter Calculations

For a flutter stability analysis aerodynamic derivatives for all combinations of Mach number and reduced frequency are required for the involved degrees-of-freedom. In the upcoming flutter experiment the heave and pitch motion, indicated by h and α respectively, will be allowed to respond freely, as the model will be mounted on a pair of torsional springs (with a stiffness of $K_\alpha = 7.282 \times 10^3$ Nm/rad) and two pairs of leaf springs ($K_h = 8.902 \times 10^5$ N/m). A detailed description of the experimental setup can be found in [4]. The wind tunnel model itself is assumed to be rigid. Figure 1 depicts a sketch of the two-DoF system. The airfoil with the mass $m = 26.252$ kg, the moment of inertia $I_\alpha = 0.0776$ kg/m², the static moment $S_\alpha = 0.2659$ kg m and

Fig. 1 Two DoF flutter model



the chord length $c = 0.3$ m is elastically mounted at its quarter chord and exposed to a flow with the free stream velocity U_∞ , so that a lift force L and a pitching moment M occur. The center of gravity is located at a distance of $x_g c$ behind the elastic axis. The DoFs are structurally damped with D_α and D_h . The equations of motion derived from this model are written in the Laplace domain as

$$[\mathbf{M}s^2 + \mathbf{D}s + \mathbf{K} - q\mathbf{SA}(\mathfrak{S}(s))] \begin{bmatrix} \hat{h} \\ \hat{\alpha} \end{bmatrix} = 0, \quad (1)$$

with $\mathbf{M} = \begin{bmatrix} m & S_\alpha \\ S_\alpha & I_\alpha \end{bmatrix}$, $\mathbf{D} = \begin{bmatrix} D_h & 0 \\ 0 & D_\alpha \end{bmatrix}$, $\mathbf{K} = \begin{bmatrix} K_h & 0 \\ 0 & K_\alpha \end{bmatrix}$ and $\mathbf{A} = \begin{bmatrix} -c_{l_h} & -c_{l_\alpha} \\ c_{m_{y_h}} & c_{m_{y_\alpha}} \end{bmatrix}$.

The Laplace variable is defined as $s = \delta + i\omega$, where δ denotes the damping and ω denotes the angular frequency. The aerodynamic matrix $\mathbf{A}(\mathfrak{S}(s))$ contains the lift and pitching moment coefficient derivatives, obtained by measurements for pitch (c_{l_α} and $c_{m_{y_\alpha}}$, Sect. 2.2) and by simulations for heave (c_{l_h} and $c_{m_{y_h}}$, Sect. 2.3). It is multiplied by the dynamic pressure q and the area S . The components of the mass matrix \mathbf{M} , the damping matrix \mathbf{D} and the stiffness matrix \mathbf{K} were obtained through weighing and a vibration test. For this model both vacuum modes are pitch dominated, with mode two containing a considerable portion of heave. The eigenfrequencies are $f = [50.4, 27.3]$ Hz and the undamped eigenvectors are $\Psi = \begin{bmatrix} -0.015 & 0.469 \\ 1.000 & 0.883 \end{bmatrix}$, read column-by-column.

In the flutter analysis the nonlinear eigenvalue problem (Eq. 1) is solved for different total pressures and Mach numbers at a constant wind tunnel temperature. A p-k-method is applied to obtain frequencies and dampings. Additionally, the eigenvectors are determined to avoid a transposition of the modes.

2.2 Forced-Motion Wind Tunnel Experiment

Forced pitch oscillations of a rectangular CAST 10-2 airfoil model [5] were measured. The model has a chord length of $c = 300$ mm and a span of $b = 997$ mm. It is equipped with 60 unsteady pressure sensors, which are arranged in one central section. 26 hot-film sensors are used to determine the condition of the boundary

layer. Additionally, the current angle-of-attack was measured by laser triangulators. The measurements were carried out with the plain airfoil (free transition) and with transition tripping dots glued to its surface at a streamwise position of $x/c = 0.075$ (fixed transition). A detailed description of the experimental set-up can be found in [7]. Measurements with a pitching amplitude of $\hat{\alpha} = 0.2^\circ$ were conducted at four different Mach numbers and at five to nine different reduced frequencies ($\omega^* = 2\pi f \frac{c}{U_\infty}$), in order to obtain the aerodynamic derivatives of the lift and pitching moment coefficient due to pitch oscillations (c_{l_α} and $c_{m_{y\alpha}}$). In addition, the mean angle-of-attack $\bar{\alpha}$ was varied, as the lift and moment curves are nonlinear over the angle-of-attack at transonic flow conditions for free transition. All measurements were conducted at a Reynolds number of $Re = 2 \cdot 10^6$.

2.3 DLM Calculations and Correction Methods

The aerodynamic response to the heave motion is not available from the current experiment and therefore has to be obtained numerically. DLM is used to perform the unsteady calculations, since it is fast and corrections can be included with comparatively little effort. The wing is modeled as a rectangular half wing with a symmetry plane. The comparison with the pressure section of the experimental results is done using the strip of DLM-boxes directly at the symmetry plane. A parameter study is conducted to obtain a grid, that minimizes the influence of the tip vortex at the inner section. This leads to a model with a semi-span of 30 chords, 16 elements in flow direction and a maximum aspect ratio of the elements of six. Thus, the wing is discretized into 1280 boxes. One advantage of DLM is the high computational efficiency. However, DLM is only reliable for subsonic, attached flow. Since DLM cannot predict viscous effects and transonic phenomena such as recompression shocks, corrections have to be introduced.

Various correction methods were developed in the past, an overview can be found in [9]. Corrections exist that are based on steady, quasi-steady or unsteady nonlinear data, which are obtained either by experiment or by CFD. In this study two different correction methods for heave DoF adjustment are applied: A direct transfer of the pitch correction matrices similar to [3] and the synthetic mode correction technique (SMC) [11]. For both methods DLM calculations for heave and pitch are performed.

For the direct transfer of the correction matrices the DLM response to a pitch motion is updated with experimental data. The approach is described for subsonic test cases in [3]: Supposing that the experimental forces are equal to the theoretical forces multiplied by a correction matrix, it is assumed that this relation holds true for the local pressure differences as well. With information about unsteady test cases for a single DoF, correction matrices are derived for various reduced frequencies and flow speeds. The obtained matrices are used to estimate the pressure distributions for all other DoF. The method was validated for subsonic test cases [3]. In the present paper this approach is modified such that the downwash w is updated by a diagonal correction matrix \mathbf{C} , so that the updated pressure distribution coincides with the

experimental data. DLM relates the downwash and the pressure distribution Δc_p through an aerodynamic influence coefficients matrix **AIC**

$$w_\alpha = \mathbf{AIC}^{DLM} \cdot \Delta c_{p_\alpha}^{DLM}. \quad (2)$$

The experimental equivalent is

$$w_\alpha = \mathbf{AIC}^{Exp} \cdot \Delta c_{p_\alpha}^{Exp} \text{ with } \mathbf{AIC}^{Exp} := \mathbf{C} \cdot \mathbf{AIC}^{DLM}. \quad (3)$$

Therefore, the elements of the diagonal correction matrix c_{ii} can be calculated as

$$c_{ii} = \frac{[w_\alpha]_i}{[\mathbf{AIC}^{DLM} \cdot \Delta c_{p_\alpha}^{Exp}]_i}. \quad (4)$$

Directly transferred to the heave results, the corrected pressure differences read:

$$\Delta c_{p_h}^{DLM,direct} = (\mathbf{C} \cdot \mathbf{AIC}^{DLM})^{-1} \cdot w_h. \quad (5)$$

Since the distribution of the pressure sensors in the wind tunnel model is finer than the aerodynamic grid of the DLM, a spline interpolation is performed to transfer the measured pressure coefficients to the DLM grid points.

The synthetic mode correction technique was developed to reduce the number of unsteady CFD calculations in terms of the number of structural modes [11]. In [2] the process was applied to a three-DoF flutter problem: At first, suitable synthetic modes have to be chosen and weighting factors have to be introduced. In the next step unsteady computations are performed for real and synthetic modes with DLM. Furthermore, unsteady calculations of the synthetic modes are carried out with a CFD solver. Finally, correction factors for each real mode, at each Mach number and reduced frequency, are obtained. When this technique is transferred to the present problem, the real modes are heave and pitch, which are calculated with DLM. The synthetic mode is pitch, which has been measured experimentally. With the weighting factors $\xi(\omega^*) = \frac{w_\alpha^H w_h}{w_\alpha^H w_\alpha}$ the corrected pressure differences are

$$\Delta c_{p_h}^{DLM,SMC} = \Delta c_{p_h}^{DLM} + \xi (\Delta c_{p_\alpha}^{Exp} - \Delta c_{p_\alpha}^{DLM}). \quad (6)$$

The method was verified at subsonic and transonic flow conditions in comparison to a CFD reference involving all DoFs [2].

3 Results

3.1 Aerodynamic Derivatives

The lift and pitching moment polars measured at $Ma = 0.75$ for free and fixed transition are shown in Fig. 2. A nonlinear segment is found for free transition in both plots. Figure 3 shows the measured unsteady derivatives of the pitching moment in magnitude and phase, exemplarily for a Mach number of $Ma = 0.75$ and three different mean pitch angles $\bar{\alpha}$. The aerodynamic response to a pitch oscillation is influenced by the mean pitch angle. For $\bar{\alpha} = -0.6^\circ$ and free transition, which corresponds to a case on the linear part of the lift polar, the progression of the curve is similar to the case with fixed transition, which was measured at $\bar{\alpha} = 1.0^\circ$. For both test points the slope of the pitching moment has a similar magnitude. A different behavior is observed at $\bar{\alpha} = 1.0^\circ$ and free transition, when the polar is at the changeover to linear. Note the phase lead of the pitching moment for all measured reduced frequencies (Fig. 3b), which indicates a possible one-DoF flutter.

The correction of the DLM results leads to differences in the local pressure distribution between free and fixed transition as found in the experiments. For $Ma = 0.5$ the effect of laminar-turbulent transition is captured in the pitch mode between $0.3 \leq x/c \leq 0.5$ as shown in Fig. 4a and transferred to the heave mode with both

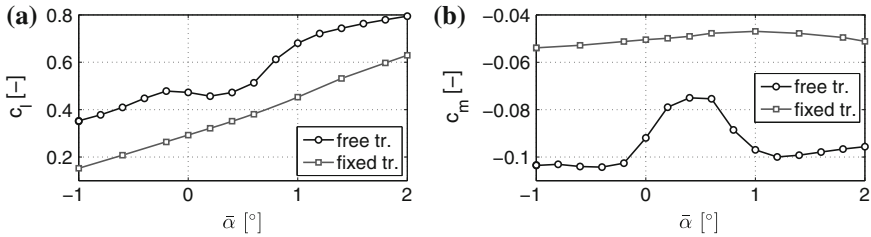


Fig. 2 Lift and pitching moment polars at $Ma = 0.75$. a Lift. b Pitching moment

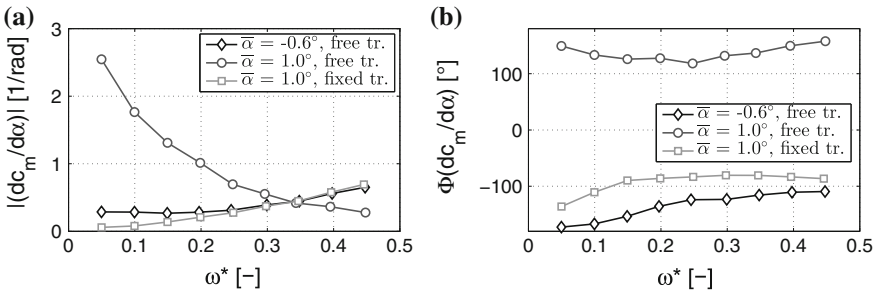


Fig. 3 Measured pitching moment derivatives due to pitch oscillations at $Ma = 0.75$ [7]. a Magnitude. b Phase

Fig. 4 Comparison of $|\Delta c_p|$ at $\omega^* = 0.05$ and $Ma = 0.5$. **a** Pitch. **b** Heave

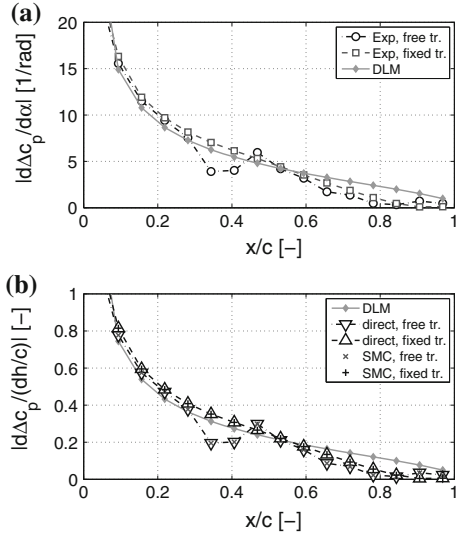
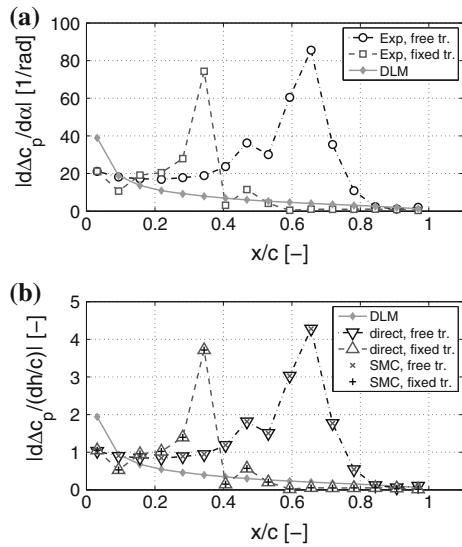


Fig. 5 Comparison of $|\Delta c_p|$ at $\omega^* = 0.05$ and $Ma = 0.75$. **a** Pitch. **b** Heave



correction methods, see Fig. 4b. For transonic Mach numbers the shock position ($x/c = 0.35$ for fixed transition and $x/c = 0.65$ for free transition) is also included in the corrections, shown for $Ma = 0.75$ in Fig. 5.

The global results of the complex-valued lift derivatives due to heave are depicted in Fig. 6 in terms of magnitude and phase for a Mach number of $Ma = 0.75$. An influence of the corrections on the magnitude is visible (Fig. 6a), with larger deviations for free than for fixed transition compared to the uncorrected DLM. Significant dif-

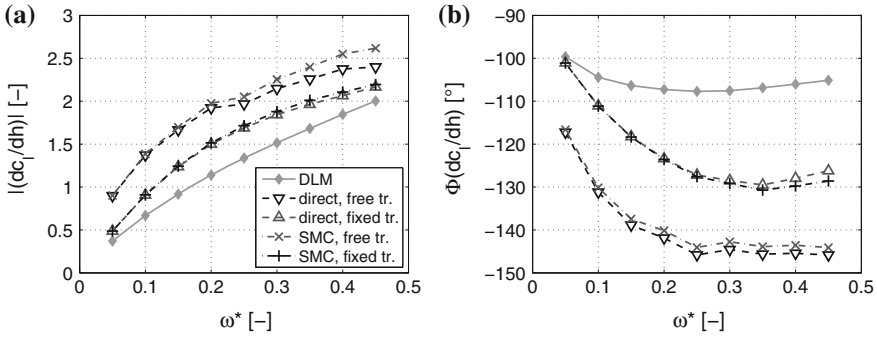


Fig. 6 Calculated lift derivatives due to heave oscillations for CAST-10 airfoil at $Ma = 0.75$. **a** Magnitude. **b** Phase

ferences can be observed in the phase of the derivatives, especially for free transition (Fig. 6b), which grow with reduced frequency. The two correction methods yield about the same derivatives for small reduced frequencies, narrow differences occur for higher reduced frequencies. Nevertheless, both approaches for heave correction agree well with each other, which supports the validity of the correction methods. At this transonic Mach number the discrepancy of the derivatives calculated with DLM and the experimental results is large in magnitude and phase for free as well as fixed transition, underlining the necessity of the corrections.

3.2 Flutter Results

The impact of the mean angle-of-attack on the flutter behavior is investigated at a flow speed of $Ma = 0.75$. For the direct transfer correction the damping, which is represented by the nondimensional logarithmic decrement $\Lambda = 2\pi \frac{\Re(s)}{\Im(s)}$, and the frequency are shown in Fig. 7 as function of the static pressure p_0 , which is the input parameter in the wind tunnel experiment. The frequencies of mode 1 vary slightly with p_0 exhibiting the biggest changes for fixed transition, while the frequencies of mode 2 are barely influenced by $\bar{\alpha}$ (Fig. 7b). On the contrary, the damping (Fig. 7a) depends strongly on $\bar{\alpha}$. For free transition and $\bar{\alpha} = -0.6^\circ$ mode 2 becomes unstable at a critical static pressure of $p_{0,crit} = 48.4$ kPa. At $\bar{\alpha} = 1.0^\circ$ mode 2 becomes unstable at a considerably lower pressure of $p_{0,crit} = 26.4$ kPa. Additionally, the first mode becomes unstable at $p_{0,crit} = 14.4$ kPa. Here the advantage of a frequency-domain over a time-domain method is demonstrated, as instabilities are found for both modes. Figure 8 depicts an analysis of the heave to pitch ratio for this angle-of-attack. It is shown that the oscillation mode 1 is pitch dominated, including only a small amount of heave. Mode 2 is also pitch dominated, but the heave portion is growing from about 50 to 65%. For both modes the phase changes from vacuum pressure to the critical flutter pressure, which indicates a coupling between the DoFs. If the system

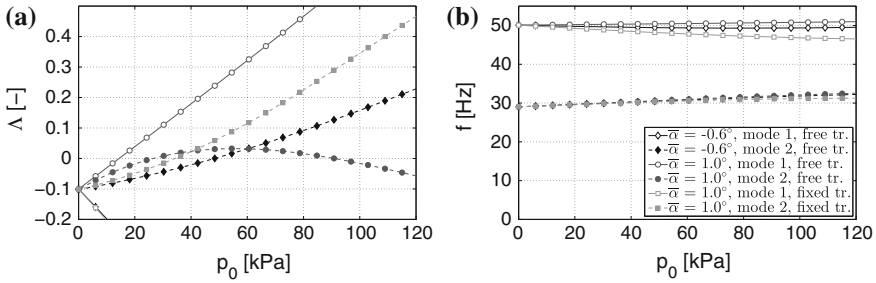


Fig. 7 Damping and frequency over static pressure for different angles-of-attack at $Ma = 0.75$ and free transition. **a** Damping. **b** Frequency

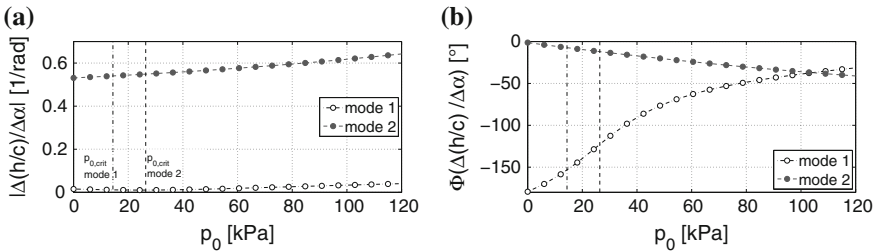
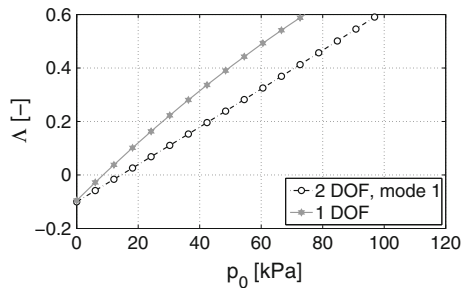


Fig. 8 Heave to pitch ratio of the aeroelastic eigenvectors over p_0 at $Ma = 0.75$, $\bar{\alpha} = 1.0^\circ$ and free transition. **a** Magnitude. **b** Phase

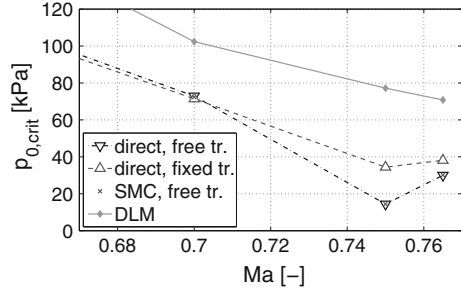
Fig. 9 Comparison of flutter models at $Ma = 0.75$ and free transition



is reduced to single DoF, an instability is predicted at a lower static pressure than the 2-DoF solution, see Fig. 9. The single-DoF flutter is consistent with the observation of the forced motion experiment, where a phase lead in the pitching moment was found (see Sect. 3.1). For fixed transition and $\bar{\alpha} = 1.0^\circ$ only the second mode becomes unstable (Fig. 7) at a higher static pressure ($p_{0,crit} = 34.4$ kPa) compared to free transition. Single-DoF flutter is not found for fixed transition.

For the comparison of the flutter boundary between laminar and turbulent flow, the critical pressures are plotted versus Mach number in Fig. 10 for $\bar{\alpha} = 1.0^\circ$. The critical

Fig. 10 Critical static pressure over Mach number at $\bar{\alpha} = 1.0^\circ$



pressures at flow speeds above $Ma = 0.7$ are lower for free transition than for fixed transition. Both curves have their minimum at $Ma = 0.75$, which is more pronounced for free transition. However, the resolution of Mach supporting points available from the experiment is too coarse to identify the exact minimum of the transonic dip of the airfoil. Furthermore, the different correction methods are compared for free transition in Fig. 10. Both predict the same critical pressures. In [2] is shown for SMC that a correction based on pitch motion only, leads to a lower stability boundary compared to calculations using all involved DoFs. This more conservative estimation of the flutter boundary reduces the risk in the upcoming wind tunnel experiment. Additionally, the results of the uncorrected DLM calculations are shown in Fig. 10. The stability boundary is located considerably above the others.

4 Conclusions

The influence of free and fixed transition on the flutter boundary is analyzed for a CAST 10-2 airfoil. The airloads are obtained from wind tunnel experiments for the pitch motion and from DLM calculations for the heave motion. Two DLM correction methods are applied, both based on experimental pitch derivatives, accounting for transonic as well as for transitional effects. A good agreement between both correction methods is obtained for the aerodynamic loads as well as for the flutter stability.

Two-DoF flutter is predicted for the considered Mach numbers ($0.5 \leq Ma \leq 0.765$) and mean angles-of-attack for both free and fixed transition. In agreement with [6, 10] the predicted flutter boundary is lower for free transition than for fully turbulent flow under transonic flow conditions. An additional instability point was found at $Ma = 0.75$ for flow with free transition. The oscillation mode is dominated by the pitch DoF including a small contribution of the heave motion. If the heave DoF is blocked, single DoF flutter is obtained at a smaller static pressure compared to the two-DoF solution. This instability is not present for fixed transition.

Regarding the preparation of the flutter experiment, the region of the transonic dip around $Ma = 0.75$ has to be investigated carefully. In future, the simulated flutter results will be compared to the experimental flutter test.

References

1. Albano, E., Rodden, W.P.: A doublet-lattice method for calculating lift distributions on oscillating surfaces in subsonic flows. *AIAA J.* **7**(2), 279–285 (1969)
2. Banavara, N.K., Dimitrov, D.: Prediction of transonic flutter behavior of a supercritical airfoil using reduced order methods. In: Dillmann, A. et al. (eds.) *New Results in Numerical and Experimental Fluid Mechanics IX. Notes on Numerical Fluid Mechanics and Multidisciplinary Design*, vol. 124, pp. 365–373. Springer International Publishing (2014)
3. Bergh, H., Zwaan, R. J.: A method for estimating unsteady pressure distributions for arbitrary vibration modes from theory and from measured distributions for one single mode. Technical report NLR-TR F.250, Feb 1966
4. Dietz, G., Schewe, G., Mai, H.: Experiments on heave/pitch limit-cycle oscillations of a supercritical airfoil close to the transonic dip. *J. Fluids Struct.* **19**(1), 1–16 (2004)
5. Dress, D.A., Mcguire, P.D., Stanewsky, E., Ray, E.J.: High reynolds number tests of the CAST 10–2/DOA 2 airfoil in the Langley 0.3-meter transonic cryogenic tunnel, phase 1. Technical report, May 1983
6. Fehrs, M.: Influence of transitional flows at transonic mach numbers on the flutter speed of a laminar airfoil. In: *Proceedings “IFASD 2013”*, Bristol, Great Britain, June 2013
7. Hebler, A., Schojda, L., Mai, H.: Experimental investigation of the aeroelastic behavior of a laminar airfoil in transonic flow. In: *Proceedings “IFASD 2013”*, Bristol, Great Britain, June 2013
8. Mai, H., Hebler, A.: Aeroelasticity of a laminar wing. In: *Proceedings “IFASD 2011”*. Paris, Frankreich (2011)
9. Palacios, R., Climent, H., Karlsson, A., Winzell, B.: Assessment of strategies for correcting linear unsteady aerodynamics using CFD or experimental results. In: *Proceedings “IFASD 2001”*, Madrid, Spain, June 2001
10. van Rooij, A.C.L.M., Wegner, W.: Numerical investigation of the flutter behaviour of a laminar supercritical airfoil. In: Dillmann, A. et al. (eds) *New Results in Numerical and Experimental Fluid Mechanics IX. Notes on Numerical Fluid Mechanics and Multidisciplinary Design*, vol. 124, pp. 33–41. Springer International Publishing (2014)
11. Voß, R., Thormann, R.: Flutter computations for a generic reference aircraft adopting CFD and reduced order methods. American Institute of Aeronautics and Astronautics (2012)